ELSEVIER

Journal of Alloys and Compounds 434–435 (2007) 60–63

Journal of ALLOYS AND COMPOUNDS

www.elsevier.com/locate/jallcom

A unified study of crack propagation in amorphous silica: Using experiments and simulations

C.L. Rountree [a,*], S. Prades [b], D. Bonamy [a], E. Bouchaud [a], R. Kalia [c], C. Guillot [a]

[a] *Service de Physique et Chimie des Surfaces et Interfaces, DSM/DRECAM/SPCSI, CEA Saclay, F-91191 Gif sur Yvette, France*
[b] *Department of Materials, Swiss Federal Institute of Technology, ETH, Hönggerberg, Wolfgang-Pauli-Strasse 10, CH-8093 Zürich, Switzerland*
[c] *Collaboratory for Advanced Computing and Simulations, Departments of Material Science and Engineering, Physics and Astronomy, Computer Science, and Biomedical Engineering, University of Southern California, Los Angeles, CA 90089-0242, USA*

Available online 20 December 2006

Abstract

Atomistic aspects of dynamic fracture in amorphous silica are investigated with molecular dynamics (MD) simulations. Simulations on amorphous silica were performed for two system sizes, 15 million and 113 million atoms. Crack propagation in these systems is accompanied by nucleation and growth of nanometer scale cavities up to 20 nm ahead of the crack tip. Cavities coalesce and merge with the advancing crack to cause mechanical failure. This scenario was also observed experimentally during stress corrosion ultra-slow fracture of glass using atomic force microscopy (F. Célarié et al., Phys. Rev. Lett. 90 (2003) 075504; S. Prades, D. Bonamy, D. Dalmas, E. Bouchaud, C. Guillot, Int. J. Sol. Struct. 42 (2004) 637). This mechanism has macroscopic consequences in terms of sample life-time and deformation field. The morphology of the fracture surfaces has also been studied by calculating the height–height correlation function. In general experiments reveal two universal roughness exponents, 0.5 for small length scales and 0.8 for large length scales. The MD simulations of the 15 million and 113 million atoms system find the first roughness exponent (0.5), but the second exponent (0.8) occurs over length scales inaccessible to MD simulations. Finally, the 113 million atoms simulation was used to map out the morphology and dynamics of the whole crack front.

Keywords: Fracture and cracks; Corrosion fatigue; Brittleness; AFM; Simulations; Silica

1. Introduction

Over the last century, a number of developments have significantly advanced our understanding of fracture at the macroscopic scale [1–4]. For several decades, fracture mechanics addressed the need for reliable safety criteria for engineering design. In recent years, the focus has shifted towards microscopic processes that occur near the crack front. Experimentally, atomic force microscopy (AFM) and scanning electron microscopy (SEM) have become a few of the tools commonly used to study fracture at the nanometer scale [5–7]. From the simulation viewpoint, molecular dynamics (MD) has become the method of choice to study fracture at the atomic scale and can easily provide atomic-level information on the dynamic features of crack propagation [8–13].

One of the most interesting and common materials to study is silicate glasses. Glasses are used everywhere from the window panes in homes to storage of nuclear waste. Furthermore, they are usually considered as a common example of "brittle" materials that break abruptly, whereas in metals, crack propagation is accompanied by plastic processes. In metallic alloys the cracks usually progress through the coalescence of damage cavities. However, MD simulation studies carried out at the Naval Oceanographic Office Major Shared Resource Center (NAVO MSRC) have revealed that, despite these dissimilarities, damage in a glass is akin to that in a metal, albeit at a much smaller length scale [8–13]. This has also been confirmed by AFM studies [5,6].

2. Computational procedure

MD simulations of silica are performed with a reliable inter-atomic potential, consisting of two-body and three-body terms [14,15]. The two-body terms contain the effects of charge–dipole, screened Coulomb, and steric repulsion. The

* Corresponding author.
E-mail address: crountree@cea.fr (C.L. Rountree).

0925-8388/$ – see front matter © 2006 Published by Elsevier B.V.
doi:10.1016/j.jallcom.2006.08.336

three-body terms is a Stillinger–Weber like potential modeling the bond bending and the bond stretching effects. The potential is validated by comparing experimental and simulations results for the bulk, shear, and Young's moduli, Poisson ratio, and the static structure factor [14,15]. The results all compare favorably.

Amorphous silica is generated by heating beta cristobalite to 3200 K. The molten system at 3200 K is first relaxed, then gradually cooled to 2500 K and allowed to relax again. Subsequently, the system is gradually cooled to 2000, 1500, 600, 300, and 5 K and allowed to relax at each intermediate step. At 5 K the conjugate-gradient method is applied to minimize the potential energy of the amorphous system. Subsequently, the glass system is heated to ambient temperature where it is further thermalized.

Tensile mode 1 fracture in MD simulations can be preformed in various ways. In general a notch is inserted by removing atoms from a specified region of the system. Subsequently, the conjugate gradient method is applied to relax the system. Another method consists of inserting a notch into a pre-strained system. Systems are strained by displacing two thin layers of atoms, located at the top and the bottom of the simulation box, in the direction of the applied strain. The strain is increased incrementally and between each increment the system is relaxed.

3. Experimental setup

Atomic force microscopy has greatly enhanced scientists' ability to probe matter at the nanoscale. The main drawback of such a technique when studying crack propagation resides in the time resolution. (The typical time to record a frame is on the order of a minute.) Therefore, the experiments presented here were performed in the ultra-slow stress corrosion regime, which enables one to track the failure mechanisms occurring at the crack tip in real time using an AFM. Fracture experiments were performed on Double Cleavage Drilled Compression specimens [5,6]. This geometry is advantageous because the stress decreases at the crack tip as the crack grows. In an inert atmosphere, the crack would then stop after having reached a given length since the load becomes too low. But, in a humid atmosphere, stretched chemical bonds are easily hydrolyzed, and break. Due to this chemically assisted mechanism, one gets velocities, v, ranging from 10^{-12} to 10^{-9} m/s, slow enough to be monitored by AFM. In this velocity regime, the crack growth rate can be controlled by adjusting the load [5,6].

4. Results

Fig. 1(a–c) shows the evolution of damage in the MD simulation from the atomic view. Crack propagation is accompanied by the nucleation and growth of nanometer scale cavities ahead of the crack tip. Cavities coalesce and merge with the advancing crack to cause mechanical failure [8]. Fig. 2 shows a snapshot of pores in the 113 million atoms system. The area around the crack front where pores nucleate is referred to as the process zone. The pore distribution around the crack front and the growth and coalescence of the pores has been studied in great detail in the 113 million atoms MD simulation since it provides a large number of statistics [13]. To show this explicitly snapshots of pores opening up in time are depicted in Fig. 3. These images are a sequence of snapshots taken in the slow region of a group of pores ahead of the crack tip. Images are separated by 4 ps. Pores are found to grow and coalesce with one another. Within 1 ps after the last image the pore merges with the crack front. Thus pores grow, coalesce, and merge with the advancing crack to cause mechanical failure.

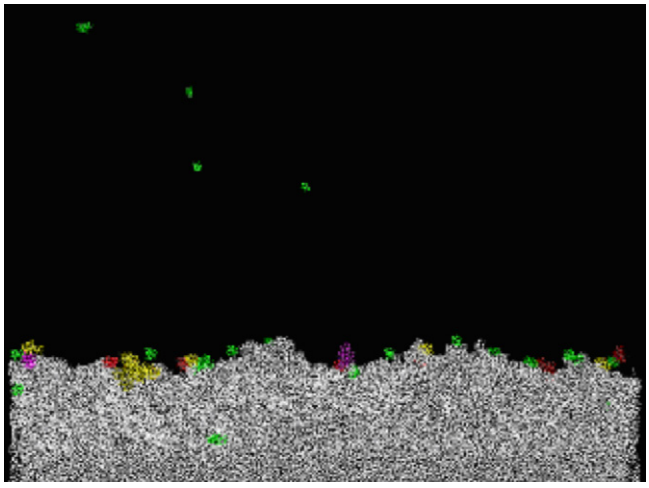

Fig. 2. Pores (colored) ahead of the crack front (white) in the 113 million atoms system.

In the 113 million atoms simulation, two velocity, v, regimes were evidenced ($v = 400$ and 1300 m/s). In these two regimes, cavities are seen to open up approximately 10–25 nm ahead of the crack tip in the slow and fast regimes, respectively. (*Note*: It should be emphasized that when the crack is propagating at 1300 m/s, the full possible extent of the zone where pores are opening is not realized due to the finite system size.)

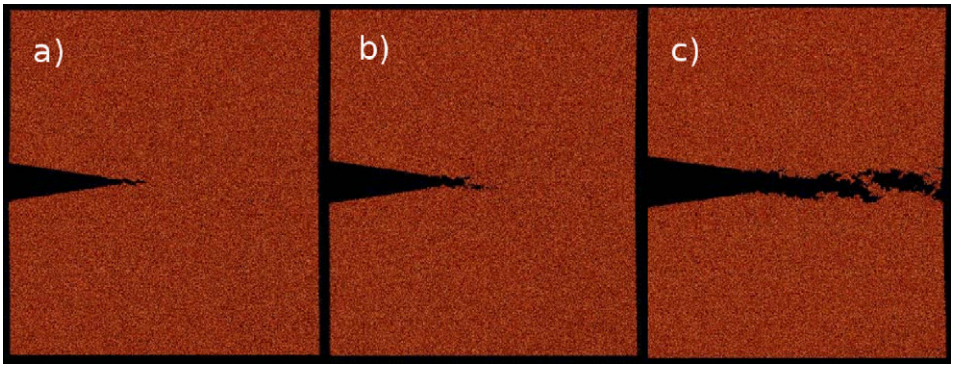

Fig. 1. Evolution of the crack in the 15 million atoms system.

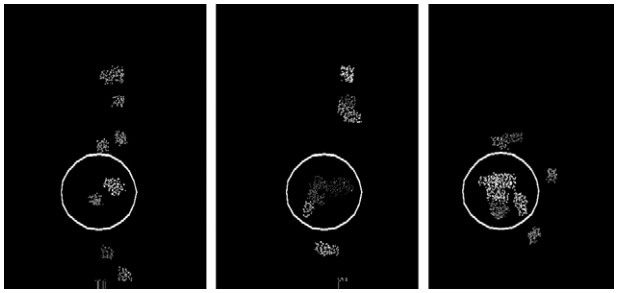

Fig. 3. Snapshots of pores in front of the notch. Frames are separated by 4.0 ps. Circle depicts a region where pores are growing and merging with other pores. After image (c) the pores merge with the crack front within 1 ps.

Experimentally, AFM studies of stress corrosion fracture in a-SiO_2 and aluminosilicate glasses also reveals nanocavitation and coalescence of cavities with the crack to be the mechanism of fracture. Fig. 4 represents a sequence of 350 nm × 350 nm AFM frames in the vicinity of the crack tip. They depict a crack in silica glass propagating at 3×10^{-11} m/s. The left image illustrates the crack front. The middle image depicts the crack propagating and a cavity opens up. Subsequently, the cavity merges with the crack front (last image) causing the crack to cross the region of interest. Thus, simulations and experiments reveal similar methods of fracture.

Due to the large number of statistics in the 113 million atoms MD simulation, the crack-front morphology and dynamics were analyzed. Fig. 5a shows the cross-correlation function of the in-plane (i.e. movements parallel to the direction of propagation) position of the crack front in the slow region averaged over all crack fronts separated by Δt, where Δt ranges from 0.5 to 12.5 ps in intervals of 0.5 ps. The function is highly correlated over a significant portion of the crack front, and the shape of the cross-correlation function remains nearly constant. The spatial-correlation function for crack front separated by 0.5 ps decays over the first 41 nm; in the interval from 4 to 31 nm the decay is linear (decreasing from 0.70 to −0.22). Between 24 and 75 nm the spatial-correlation function is anti-correlated and reaches a minimum value of −0.39 around 41 nm. Beyond 75 nm the cross-correlation function becomes positive again, though the maximum height of the correlation is only 0.12. Similar results are seen for crack fronts separated by $\Delta t = 12.5$ ps. As time progresses the temporal correlations

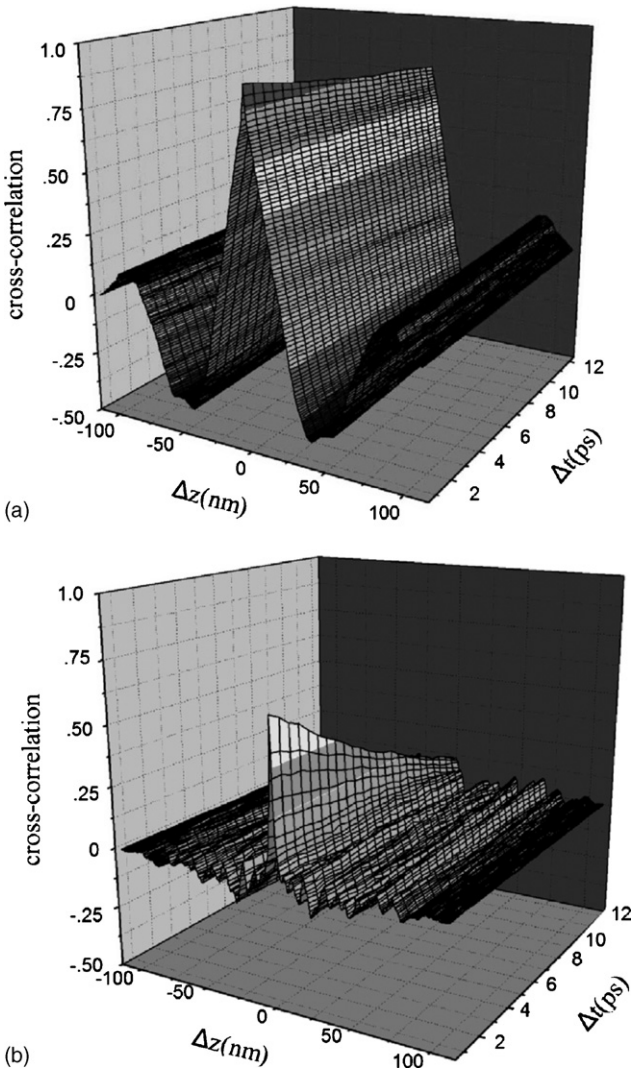

Fig. 5. Cross-correlation functions at 300 m/s. (a) In-plane cross-correlation: the crack fronts were observed to be spatially and temporally correlated. (b) Out-of-plane cross-correlation: the out-of-plane cross-correlations of the crack fronts in the slow and fast region were found to be minimal.

for $\Delta z = 0$ nm decreases from 0.91 at 0.5 ps to 0.77 at 12.5 ps which corresponds to a rate of 0.012 ps^{-1}. Thus, in-plane displacements of the crack front are both spatially and temporally correlated.

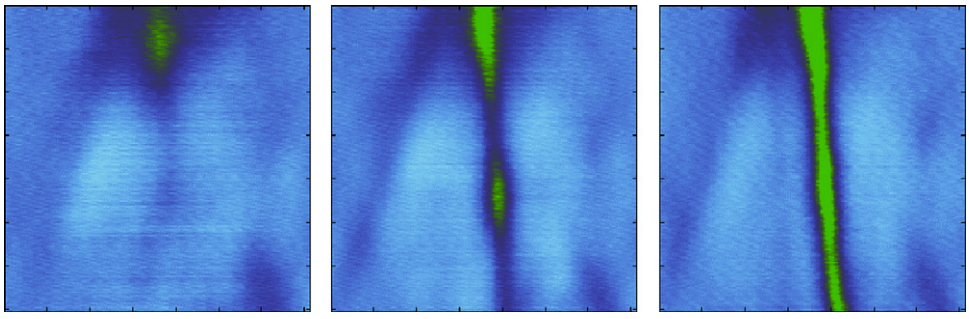

Fig. 4. AFM image of a crack propagating in silica glass. Left image: the initial crack front (shown in green); middle image: a pore opening up ahead of the crack front; right image: the crack front has merged with the pore ahead of itself and is out of view of this image. (For interpretation of the references to color in this figure legend, the reader is referred to the web version of this article.)

The cross-correlation function of the out-of-plane (i.e. movements perpendicular to the direction of propagation) crack front displacement in the slow region is shown in Fig. 5b. For crack fronts separated by 0.5 ps, the cross-correlation starts at 0.63, crosses 0 around 9 nm, and then fluctuates around zero. However, as time progresses spatial coherence in the cross-correlation curve decreases. For crack fronts separated by 12.5 ps the cross-correlation function is only 0.10 at $\Delta z = 0$ nm. This is within the fluctuations of the cross-correlation function. As a function of time, it is observed that the main peak in the spatial cross-correlations (i.e. $\Delta z = 0$ nm) decreases from 0.63 ($\Delta t = 0.5$ ps) to 0.10 ($\Delta t = 12.5$ ps). Thus, out-of-plane displacements of the crack front are not highly spatially and temporally correlated.

The morphology of fracture surfaces reveals scaling behavior akin to that observed experimentally. Fracture surfaces are self-affine objects characterized by a height–height correlation function scaling as [16,17]:

$$\Delta h(r) = \langle \max(h(x'))_{x<x'<x+r} - \min(h(x'))_{x<x'<x+r} \rangle_x \propto r^{\varsigma}$$

where $\max(h(x'))$ and $\min(h(x'))$ denote the maximum and the minimum height, respectively, of the fracture profile in the window $x < x' < x + r$, $\langle \cdot \rangle_x$ implies an average over x, and ς denotes the roughness exponent. Fracture experiments on various metals, alloys, ceramics, and glasses reveal two exponents -0.5 at small length scales and 0.8 above a crossover length, ξ_c, which decreases with an increase of the crack velocity. In both the 15 million and 113 million atoms simulations, the roughness exponent was found to be $\varsigma \approx 0.5$. The large exponent is unobtainable thus far in simulations due to system sizes.

5. Conclusion

Simulations of dynamic fracture in amorphous silica reveal that crack propagation is accompanied by nucleation and growth of nanometer scale cavities up to 20 nm ahead of the crack tip. These cavities coalesce and merge with the advancing crack to cause mechanical failure. This scenario is consistent with what was observed experimentally during stress corrosion ultra-slow fracture of glass using atomic force microscopy [5,6]. In the slow regime ($v = 400$ m/s) of MD simulations of dynamic fracture, the in-plane cross-correlations of the crack fronts were observed to be spatially and temporally correlated. However, the spatial and temporal correlations of the out-of-plane displacements of the crack fronts in the slow region were found to be minimal. In general, experiments reveal two universal roughness exponents, 0.5 for small length scales and 0.8 for large length scales. The MD simulations of the 15 million and 113 million atoms system find the first roughness exponent (0.5), but the second exponent (0.8) occurs over length scales inaccessible to MD simulations.

References

[1] A.A. Griffith, Philos. Trans. R. Soc. Lond. A221 (1920) 163.
[2] E. Orowan, Energy Criteria Fracture 34 (1955) 157.
[3] G.R. Irwin, in: S. Flügge (Ed.), Handbuch der Physik, vol. 6, Springer, Berlin, 1958, p. 551.
[4] L.B. Freund, Dynamic Fracture Mechanics, Cambridge University Press, Cambridge, 1990.
[5] F. Célarié, et al., Phys. Rev. Lett. 90 (2003) 075504.
[6] S. Prades, D. Bonamy, D. Dalmas, E. Bouchaud, C. Guillot, Int. J. Sol. Struct. 42 (2004) 637.
[7] X.K. Xi, et al., Phys. Rev. Lett. 94 (2005) 125510.
[8] C.L. Rountree, R.K. Kalia, A. Nakano, P. Vashishta, NAVO MSRC Navigator 10–11 (Fall) (2002).
[9] C.L. Rountree, et al., in: P. Vincenzini (Ed.), Proceedings of CINTEC 2002, 10th International Ceramic Congress and 3rd Forum on New Materials, Florence, Italy, 2002.
[10] L. Van Brutzel, et al., Mater. Res. Soc. Symp. Proc. 703 (2002) V.3.9.1–V.3.9.6.
[11] C.L. Rountree, et al., Annu. Rev. Mater. Res. 32 (2002) 377.
[12] R.K. Kalia, et al., Int. J. Frac. 121 (2003) 71.
[13] C.L. Rountree, Ph.D. Thesis, Louisiana State University, 2003.
[14] P. Vashishta, R.K. Kalia, J.P. Rino, I. Ebbsjo, Phys. Rev. B 41 (1990) 2197.
[15] P. Vashishta, et al., in: M.F. Thorpe, M.I. Mitkova (Eds.), Amorphous Insulators and Semiconductors, Kluwer Academic, The Netherlands, 1997, p. 151.
[16] P. Daguier, S. Hénaux, E. Bouchaud, F. Creuzet, Phys. Rev. E 53 (1996) 5637.
[17] E. Bouchaud, J. Phys. Condens. Matter 9 (1997) 4319.